WL-TR-91-2071

INTERCHANGEABLE VARIABLE CONDUCTANCE HEAT PIPES FOR SODIUM-SULFUR BATTERIES

John R. Hartenstine

Thermacore, Inc.
780 Eden Road
Lancaster, PA 17601

August 1991

Final Report for period August 1990 - June 1991

Approved for public release; distribution is unlimited.

AERO PROPULSION & POWER DIRECTORATE
WRIGHT LABORATORY
AIR FORCE SYSTEMS COMMAND
WRIGHT-PATTERSON AIR FORCE BASE, OHIO 45433-6563

REPORT DOCUMENTATION PAGE

Form Approved OMB No. 0704-0188

1a. REPORT SECURITY CLASSIFICATION: Unclassified	1b. RESTRICTIVE MARKINGS
2a. SECURITY CLASSIFICATION AUTHORITY	3. DISTRIBUTION/AVAILABILITY OF REPORT: Approved for public release; distribution is unlimited.
2b. DECLASSIFICATION/DOWNGRADING SCHEDULE	
4. PERFORMING ORGANIZATION REPORT NUMBER(S)	5. MONITORING ORGANIZATION REPORT NUMBER(S): WL-TR-91-2071
6a. NAME OF PERFORMING ORGANIZATION: Thermacore, Inc. / 6b. OFFICE SYMBOL (If applicable): 1T434	7a. NAME OF MONITORING ORGANIZATION: Aero Propulsion & Power Dir. (WL/POOS) Wright Laboratory
6c. ADDRESS (City, State, and ZIP Code): 780 Eden Road, Lancaster, PA 17601	7b. ADDRESS (City, State, and ZIP Code): Wright-Patterson AFB, Ohio 45433-6563
8a. NAME OF FUNDING/SPONSORING ORGANIZATION: Aero Propulsion & Power Dir. / 8b. OFFICE SYMBOL (If applicable): WL/POOS	9. PROCUREMENT INSTRUMENT IDENTIFICATION NUMBER: F33615-90-C-2073
8c. ADDRESS (City, State, and ZIP Code): Wright Laboratory, Wright-Patterson AFB, OH 45433-6563	10. SOURCE OF FUNDING NUMBERS: PROGRAM ELEMENT NO. 65502F; PROJECT NO. 3005; TASK NO. 21; WORK UNIT ACCESSION NO. 83

11. TITLE (Include Security Classification)
Interchangeable Variable Conductance Heat Pipes for Sodium-Sulfur Batteries

12. PERSONAL AUTHOR(S)
Hartenstine, John Richard

13a. TYPE OF REPORT	13b. TIME COVERED	14. DATE OF REPORT (Year, Month, Day)	15. PAGE COUNT
Final	FROM 90/8 TO 91/6	August 1991	47

16. SUPPLEMENTARY NOTATION

17. COSATI CODES			18. SUBJECT TERMS (Continue on reverse if necessary and identify by block number)
FIELD	GROUP	SUB-GROUP	Variable conductance heat pipe, sodium-sulfur battery, titanium, cesium, passive, interchangeable

19. ABSTRACT (Continue on reverse if necessary and identify by block number)

Sodium-sulfur batteries can provide electrical power to satellite instrumentation operating in geosynchronous-earth-orbit (GEO) and low-earth-orbit (LEO) conditions. While on orbit, the sodium-sulfur battery requires thermal management as the battery is cycled between discharge in solar eclipse and recharge in sunlight. As the battery discharges in solar eclipse waste heat is generated and the battery requires cooling. During recharge in sunlight the battery temperature needs to be maintained above 320°C.

In this Phase I program, Thermacore developed and demonstrated a dual titanium/cesium heat pipe to provide passive, lightweight management of the battery during orbital cycling. The dual heat pipe concept uses both constant and variable conductance heat pipes. Constant conductance heat pipes are inserted between sodium-sulfur cells. The cells radiate to the constant conductance heat pipes and this energy is transferred to a variable conductance heat pipe and radiated to deep space.

OVER

20. DISTRIBUTION/AVAILABILITY OF ABSTRACT	21. ABSTRACT SECURITY CLASSIFICATION
☒ UNCLASSIFIED/UNLIMITED ☐ SAME AS RPT. ☐ DTIC USERS	Unclassified

22a. NAME OF RESPONSIBLE INDIVIDUAL	22b. TELEPHONE (Include Area Code)	22c. OFFICE SYMBOL
Hager, Brian G.	(513) 476-4428	WL/POOS

Thermacore fabricated and tested a six (6) heat pipe assembly using five (5) constant and one (1) variable conductance heat pipes to verify the thermal management concept. During simulated LEO orbital cycling, the heat pipe demonstrated a 33°C temperature control range as the heat pipes cycled between $Q_{minimum}$ and $Q_{maximum}$ heat rejection conditions. This program also demonstrated how the heat pipes are interchangeable for different orbital missions such as GEO and LEO. By establishing an interchangeable thermal management design using heat pipes, the need to re-design and develop separate cooling concepts for each battery configuration is eliminated and thereby reduces battery development costs.

NOTICE

When Government drawings, specifications, or other data are used for any purpose other than in connection with a definitely Government-related procurement, the United States Government incurs no responsibility or any obligation whatsoever. The fact that the government may have formulated or in any way supplied the said drawings, specifications, or other data, is not to be regarded by implication, or otherwise in any manner construed, as licensing the holder, or any other person or corporation; or as conveying any rights or permission to manufacture, use, or sell any patented invention that may in any way be related thereto.

This report is releasable to the National Technical Information Service (NTIS). At NTIS, it will be available to the general public, including foreign nations.

This technical report has been reviewed and is approved for publication.

BRIAN G. HAGER
Project Engineer
Thermal Technology

JERRY E. BEAM, TAM
Thermal Technology
Power Technology Branch

FOR THE COMMANDER

WILLIAM U. BORGER
Chief, Aerospace Power Division
Aero Propulsion & Power Directorate

If your address has changed, if you wish to be removed from our mailing list, or if the addressee is no longer employed by your organization please notify WL/POOS , WPAFB, OH 45433-6563 to help us maintain a current mailing list.

Copies of this report should not be returned unless return is required by security considerations, contractual obligations, or notice on a specific document.

PREFACE

The technical monitor for the Phase I SBIR program was Mr. Brian Hager (WRDC). Mr. Hager was responsible for outlining the technical program to develop heat pipes to cool sodium-sulfur batteries, and supplied Thermacore with battery requirements, applications and input as to chief development areas.

This work presented herein represents the efforts of the Development Division of Thermacore, Inc. Messrs Peter M. Dussinger and Robert M. Shaubach provided technical and managerial direction on the program. Direct project engineering was supplied by Messrs John R. Hartenstine and James E. Bogart, who worked with Mr. David L. Muth in performance of the actual program hardware fabrication and testing.

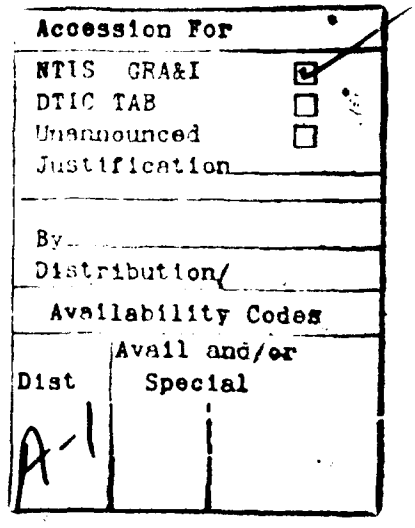

TABLE OF CONTENTS

LIST OF FIGURES

LIST OF TABLES

1.0 INTRODUCTION

Sodium-sulfur batteries are used to provide electrical power to satellite systems when the satellite is in solar eclipse. Solar receivers provide electricity to recharge the sodium-sulfur battery and supply electrical power to the remaining satellite systems in sunlight operation.

In a single orbit, the sodium-sulfur battery operation will experience an endothermic and an exothermic reaction. The endothermic reaction occurs during battery recharge in the sunlight mode of operation. In eclipse, the discharge mode of operation, an exothermic reaction takes place causing an increase in battery temperature. Accumulation of this waste heat can shorten battery life through degradation of cells and damage to the electrical components on board the satellite.

One industry approach to the thermal management of the sodium-sulfur batteries for geosynchronous-earth-orbit (GEO) and possibly low-earth-orbit (LEO) is to incorporate a mechanical louver onto the bottom of the battery casing. This louver can be operated using a stepper motor. The louver is closed during recharge operation to insulate the battery package and opened to deep space during discharge operation to radiate the generated heat.

The main disadvantage of the louver concept is in the reliability of the mechanical linkages and gears required for operation. If operated in LEO, the louver concept would be required to open and close 13 times in a 24 hour period or approximately 50,000 times in its required 10 year lifetime. If the gears or linkages become stuck the entire battery will be damaged resulting in a single point failure.

Thermacore proposed to design both constant and variable conductance titanium/cesium heat pipes (VCHP) fabricated from titanium and using cesium as the working fluid into the sodium-sulfur battery to provide passive, lightweight thermal management during orbital cycling. The dual heat pipe assembly transfers power radiated from the battery cells during discharge to constant conductance heat pipes mounted between each set of four sodium-sulfur cells. The constant conductance heat pipes transfer the power to an integral VCHP which increases the VCHP working fluid vapor pressure and temperature and pushes the control gas into a gas reservoir. This exposes the active portion of the heat pipe condenser, where the waste energy is radiated to deep space. In recharge, the power rejected from the cells decreases which

decreases the vapor pressure within the VCHP and subsequently expands the control gas which blankets the radiator. The VCHP can be designed to operate within a given set point temperature range as the battery cycles between discharge and recharge. For this application a 20°C temperature control range was selected (350°C to 370°C).

In this particular design the dual heat pipe concept uses five (5) constant conductance heat pipes and one (1) VCHP to cool eighteen (18) sodium-sulfur battery cells. Therefore, for a seventy-two (72) cell battery, 4 dual heat pipe assemblies would be needed. This adds a redundancy factor to the design. Should a single assembly be damaged by meteoroid or space debris the remaining assemblies will aid in transferring the waste heat from the un-cooled battery cells.

The constant conductance heat pipes are designed into the battery to help assure that the ceramic electrolyte within the individual sodium-sulfur cells operates with a low temperature drop along its axis. This is needed because the hottest region within the ceramic electrolyte will draw more current than the cooler regions. The area of highest current concentration will cause the electrolyte to degrade faster with respect to the remaining cell and decrease the battery cell life.

Other heat pipe concepts have been proposed to do exactly what Thermacore has proposed except the Thermacore design includes one added feature; interchangeability between GEO and LEO. This feature establishes one sodium-sulfur battery cell geometrical configuration for GEO, LEO or other orbital conditions. The heat pipe design will also be of a generic configuration such that it can be mounted within the standard sodium-sulfur battery cell arrangement. If a sodium-sulfur battery is needed for GEO, mount the GEO cells into the standardized battery enclosure. The heat pipes designed for GEO would be mounted with the GEO cells. The same procedure is used for LEO or other orbital conditions. Therefore, the need to design a separate battery packaging scheme for each orbital mission is eliminated thereby saving development costs.

In this Phase I program, Thermacore developed and demonstrated an integrated dual heat pipe concept using variable and constant conductance heat pipes to cool 18 sodium sulfur battery cells. Figure 1 shows a photograph of the assembly. The results of this work show that a 33°C temperature control range was achieved as the heat pipe was cycled through simulated LEO sodium-sulfur cell heat rejection conditions. Phase II will extend this work by designing the assembly to be lightweight using alternative heat pipe envelope and fin materials.

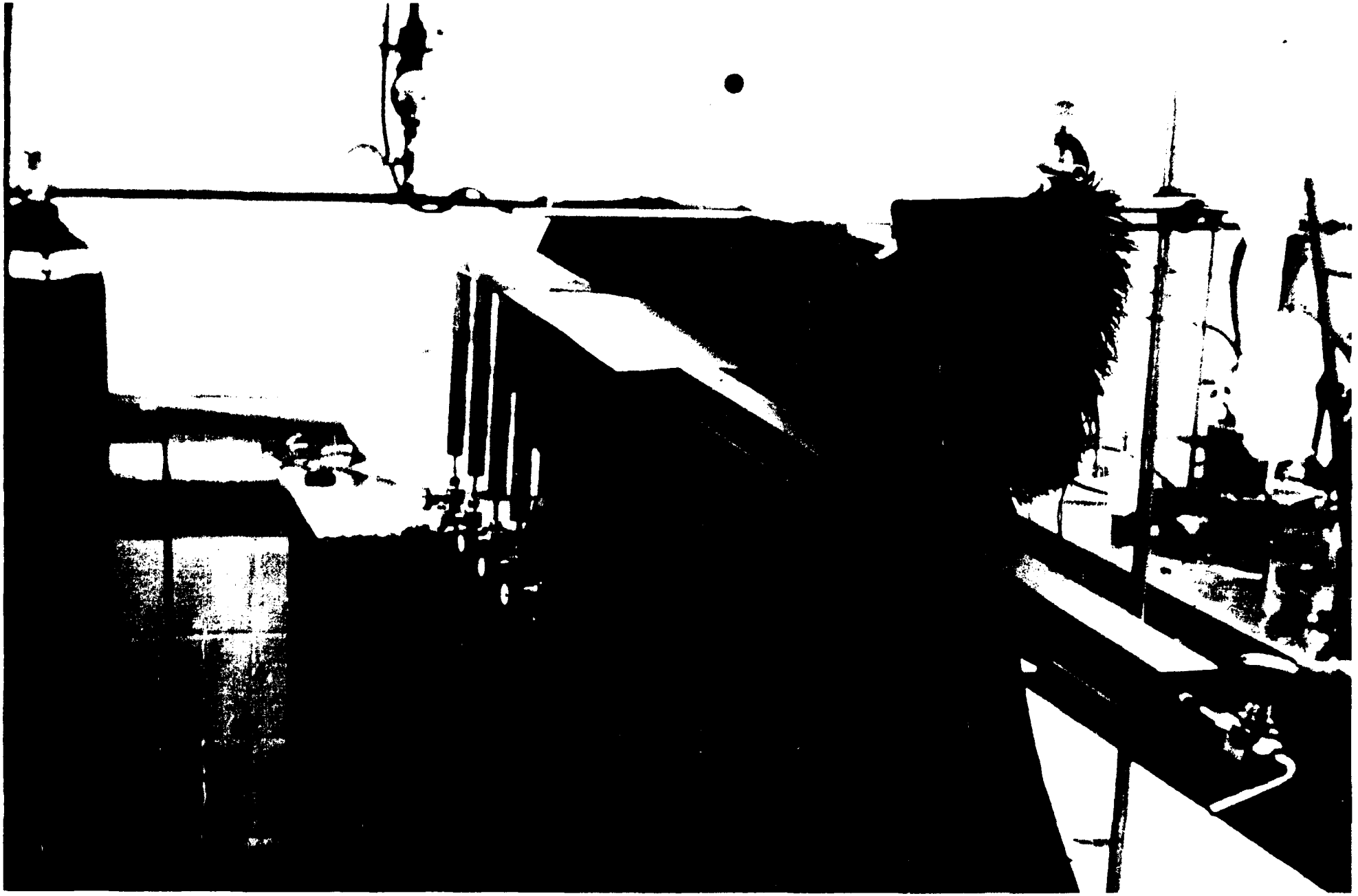

Figure 1. Variable Conductance Heat Pipe/Battery Cell Heat Pipe Assembly for Cooling Sodium-Sulfur Battery

2.0 TECHNICAL APPROACH

The technical approach for this Phase I program was divided into four (4) tasks. A description of these tasks are as follows:

- Task 1.0 Identification of the Requirements

  The thermal management design criteria for cooling sodium-sulfur batteries for operation in a low-earth-orbit (LEO) were established in a meeting between WRDC (B. Hager) and Thermacore (J. Hartenstine, P. Dussinger). The design criteria are presented in Section 3.1.

- Task 2.0 Prototype VCHP Design

  The thermal management of LEO sodium-sulfur batteries will use a dual heat pipe assembly fabricated from constant and variable conductance heat pipes. In this task the variable conductance heat pipe was designed and the details are presented in Section 3.2.

- Task 3. Battery Cell Heat Pipe Design

  The constant conductance heat pipes used in the thermal management design are positioned within the sodium-sulfur battery cells to transport waste heat and isothermalize the cells. The design details of the battery cell heat pipes (BCHP) are discussed in Section 3.3.

- Task 4. VCHP/BCHP Fabrication and Test

  The constant and variable conductance heat pipes were fabricated and tested during Task 4. The results are shown in Section 3.4.

2.1 TASK 1: IDENTIFICATION OF THE REQUIREMENTS

The design requirements for the dual heat pipe to provide thermal management of sodium-sulfur batteries for LEO were established in a meeting held at WRDC on August 29, 1990. Attending the meeting were WRDC (B. Hager) and Thermacore (J. Hartenstine,

P. Dussinger). Table 1 lists the LEO sodium-sulfur battery cell parameters which set the heat pipe design requirements.

Figure 2 shows LEO sodium-sulfur cell heat dissipation rates as a function of time during orbital cycling. At the beginning of discharge the heat dissipation is 35 watts. At the end of discharge, the cells reach a 45 watt peak and drop to 5 watts over the next 7 minutes. The heat dissipation is reduced further to 2 watts and levels off at 7 watts until the next discharge cycle takes place.

TABLE 1. Sodium-Sulfur Battery Requirements for LEO Configuration

Parameter	Magnitude
Cell Diameter	1.396 inches
Cell Length	10.5 inches
Cells per Battery	72
Battery Dimensions	18.35" x 10.6" x 12"
Discharge Time	35 minutes
Heat Dissipation per Cell	35 watts average, 45 watts peak (see Figure 2)
Total Power Rejected During Discharge (Peak)	3240 watts
Heat Leak	Minimize
Operational Temperature Range	320-390°C, 350°C Nominal
Weight	Minimize
VCHP Temperature Control Range	20°C
Number of VCHP's per Battery	4
Power Rejected During Discharge per VCHP	810 watts

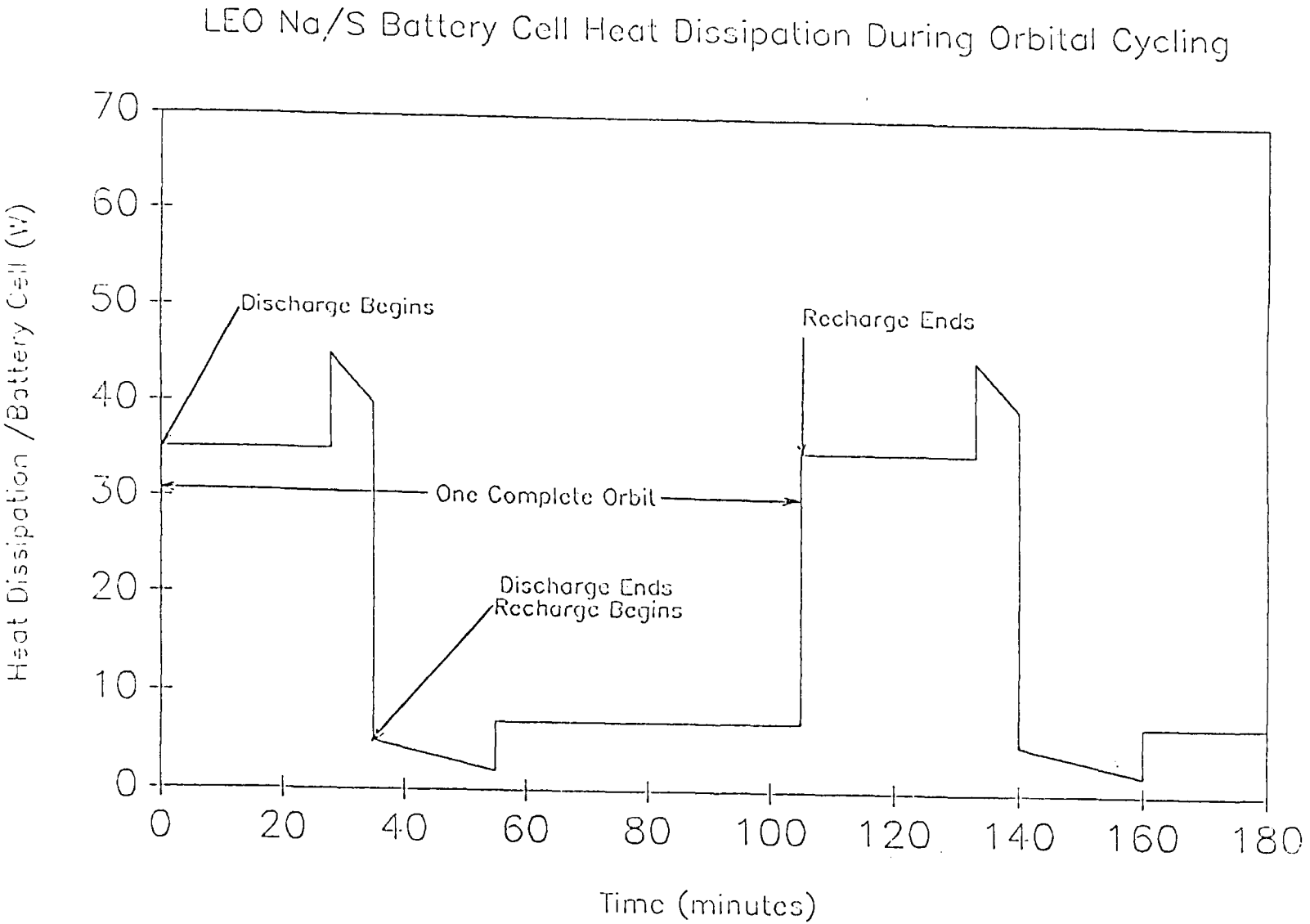

Figure 2. LEO Na/S Battery Heat Dissipation Profile During Orbital Cycling

2.2 TASK 2: PROTOTYPE VCHP DESIGN

The prototype VCHP used titanium (CP-Grade 2) as the envelope material and cesium as the working fluid. The wick structure was axial grooves. Axial grooves were selected over screen or sintered power metal wicks because these non-grooved wicks have a high liquid pressure drop that exceeds their capillary pumping capability. Sintered powder metal wicks with arteries would reduce these high liquid pressure drops, but the uncertain reliability of arteries with alkali metal working fluids disqualified these wicks. The remaining VCHP design requirements are listed in Table 2.

The VCHP geometry is a square cross section 1.575 inches x 1.575 inches x .060 inch wall. The square cross section was selected over a circular cross-section because the special tooling required to form the axial grooves on the inside diameter of circular titanium tubing was not available on Phase I funds or schedule. Instead, the grooves were milled into flat titanium plates forming the four walls of the heat pipe. The four walls with machined grooves were joined by electron beam welding.

A cross-section of the VCHP groove geometry is shown in Figure 3. The open channel grooves were partially covered with titanium screen in the evaporator and condenser. The screen reduces the liquid pressure drop that is induced by the liquid counterflow shearing effect of vapor on the liquid surface.[1] The grooves were not completely covered with screen so that vapor and/or noncondensible gas trapped in the grooves could vent to the vapor space. The addition of the screen also reduced the potential of liquid entrainment occurring during VCHP operation.

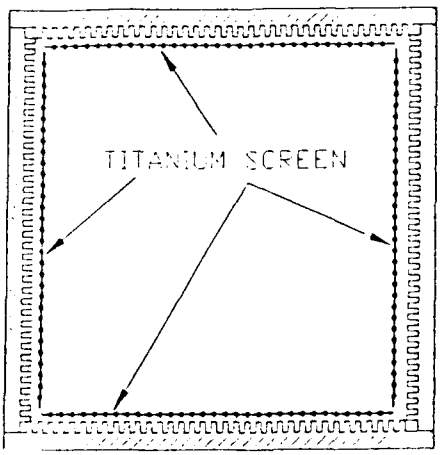

Figure 3. Screen Covered Axial Groove Wick Design

TABLE 2. Variable Conductance Heat Pipe Design Parameters for a LEO Sodium-Sulfur Battery

Envelope and End Cap Material	Titanium, CP-Grade 2
Working Fluid	Cesium
Wick Structure	Axial Grooves
- Groove Width	0.020 inches
- Groove Depth	0.040 inches
- Groove Land	0.020 inches
Operational Temperature	350°C
Sink Temperature	14°C (on earth)
Temperature Control Range	20°C (350°C-370°C)
Condenser and Reservoir Emissivity	0.80
Discharge - Recharge Time Cycle	See Figure 2
- Total Discharge Time	35 minutes
- Total Recharge Time	70 minutes
Calculated Reservoir-to-Condenser Volume Ratio	2.06:1
VCHP Geometry	See Figure 3
- Evaporator Length	22.85 inches
- Condenser Length	17.00 inches
- Reservoir Length	35.11 inches
- Fin Length	17.00 inches
- Fin Width	2.50 inches
- Fin Thickness	0.060 inches
Total VCHP Length	74.96 inches
Calculated Heat Leak	25 Watts
Diffusion Zone Length	7 inches
Calculated Weight including Cesium	2967 grams (6.5 lbs.)
Testing Orientation	Horizontal

The nominal operating temperature for the VCHP evaporator was 350°C during recharge, which is the battery mode of operation when the waste heat energy dissipation per cell is at a minimum. The control gas in the heat pipe blankets the condenser region, limiting the radiator area and thereby maintaining the battery cell temperature. When the battery discharges in solar eclipse, the waste heat energy dissipated per cell reaches a maximum. The increase in power to be rejected causes the control gas to be pushed into a gas reservoir and exposes the condenser region so the additional waste heat can be rejected. The size of the reservoir and the amount of the gas charge determine the evaporator temperature at this maximum heat loss. The VCHP was designed so that the evaporator temperature did not exceed 370°C. The temperature differential between the minimum and maximum heat loss is 20°C and is defined as the VCHP temperature control range.

Table 3 shows the power dissipation requirements for each VCHP during LEO. During orbital cycling (Refer to Figure 2) each VCHP will radiate a maximum of 810 watts (Discharge) and a minimum of 36 watts (recharge). Each VCHP is designed to cool 18 cells, therefore 4 VCHP's are required for each 72 cell LEO battery.

The VCHP uses argon to blanket the radiator section of the heat pipe during the battery recharge mode. This gas blanket prevents battery thermal energy from being dissipated unnecessarily. The heat pipe cesium vapor will diffuse into the argon blanket and tend to reduce its effectiveness. The following paragraph describes an effort to predict the amount of cesium diffusion.

TABLE 3. VCHP Power Requirements During Orbital Cycling for a 72 Cell LEO Sodium-Sulfur Battery

Q_{cell} Heat Dissipation Per Cell	Discharge / Recharge	Q_{VCHP} Heat Transport Capability of each VCHP (Watts)*
35 Watts	Discharge	630
45 Watts	Discharge	810
5 Watts	Recharge	90
2 Watts	Recharge	36
7 Watts	Recharge	126

* Each VCHP will cool 18 battery cells: $Q_{VCHP} = 18 \times Qcell$

A computer code was used to predict the length and rate of cesium vapor diffusion into the argon cover gas. Results from this analysis are used to estimate the argon reservoir volume required to achieve the proper VCHP temperature control range. If the amount of diffusion is high for example, the reservoir volume will need to be made larger than it would be if diffusion were negligible.

The computer code, developed for the GEO sodium-sulfur battery in the previous 1988 Phase I program, was modified for this LEO application. The computer code used in the previous Phase I program assumed that the temperature of the cesium vapor and argon gas in the vapor core of the reservoir remained constant at 370°C, and that the diffusion coefficient also remained constant at this temperature. While the model agreed reasonably well with the experimental results, Thermacore revised the code to take into account a non-uniform axial temperature profile in the vapor core due to thermal conductivity and radiation from the VCHP walls. The diffusion coefficient calculation was also upgraded to calculate the coefficient as a function of temperature.

The computer code was used to calculate the rate of diffusion of cesium vapor into the argon concurrent with the energy transfer by axial conduction in the pipe wall and radiation to the sink. The model assumes: no vapor inertial effects (no turbulence in the vapor core), all vapor in the nodes next to the wall condenses, all energy transfer in the core is by mass transfer and conduction. The cesium concentration was calculated as a function of reservoir length and had a convergence criteria of $1x10^{-6}$ kg/m^3. The VCHP wall temperature was calculated as a function of reservoir length and had a convergence criteria of 0.01K. A copy of the model analysis is included in Appendix A.

Two diffusion cases were run, as follows: The first case incorporated a baffle into the vapor core to reduce the amount of cesium diffusion into the reservoir. The baffle was positioned at the junction between the condenser and reservoir interface as shown in Figure 4. The second case was similar to the first without a vapor core baffle.

Table 4 shows the results from these two cases. The heat leak difference between the two cases is only 0.5 watts, indicating that the heat leak is mainly a function of the axial conduction down the wall, and not the diffusion of the cesium.

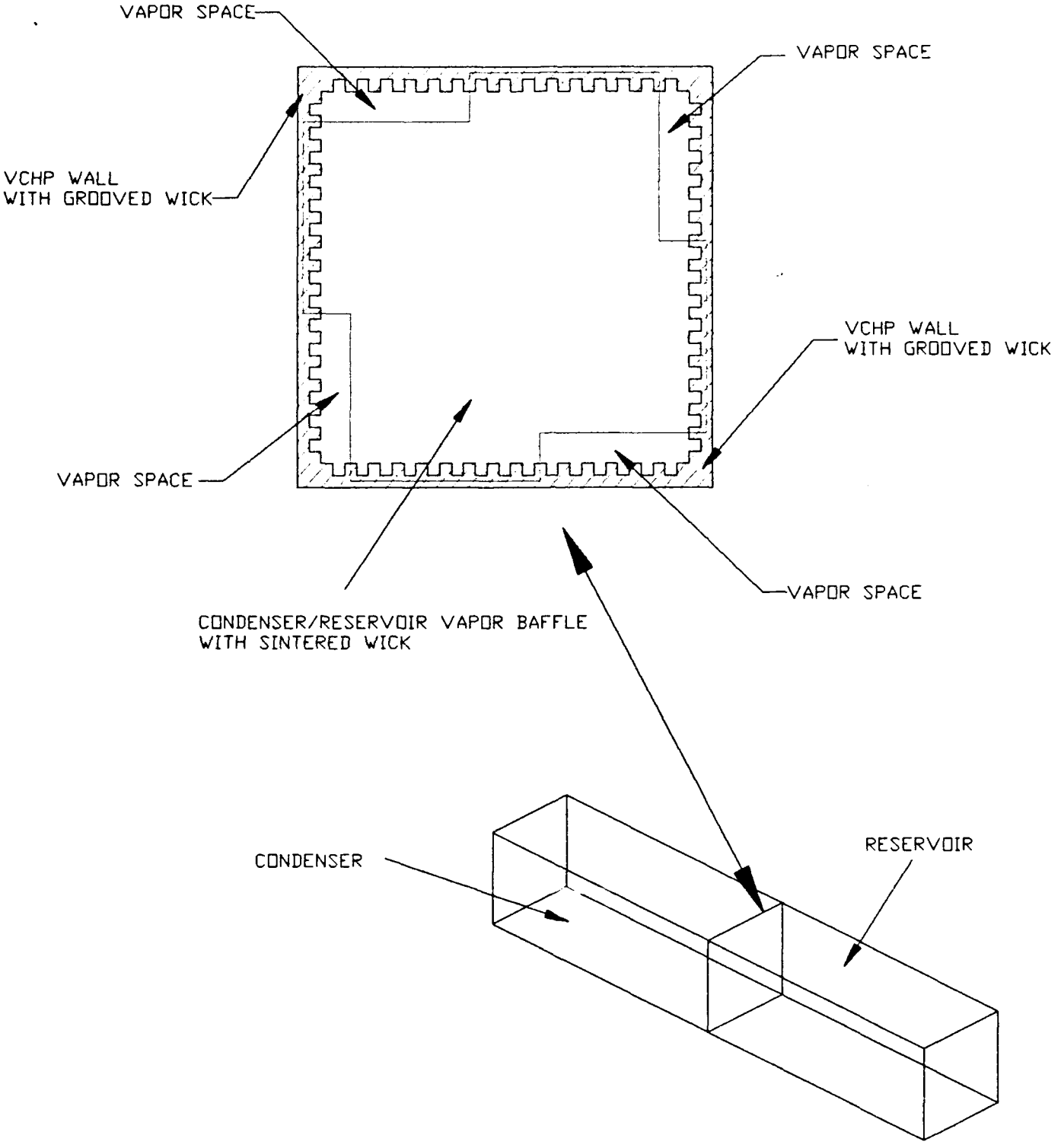

FIGURE 4. CONDENSER/RESERVOIR VAPOR BAFFLE

C:\ACAD386\11-1105\VAPORBFL.DWG

TABLE 4. Diffusion of Cesium into the Reservoir Calculation Results

Baffle Y-Yes N-No	Heat Leak (W)	Diffusion Zone Volume (in3)	Cesium Volume in Diffusion Zone (in3)	Argon Volume in Diffusion Zone (in3)
Y	23.6	12.28	1.20	11.08
N	24.1	13.23	3.24	9.99

Table 4 also shows that twice the volume of cesium will diffuse into the reservoir without a baffle than with a baffle. Even though the difference in cesium volume between the two cases seems large for this region of the heat pipe, the overall reservoir length difference (-1.08 inches) was not significant enough to warrant including a baffle into the design. Therefore, the VCHP did not use a vapor core baffle. Table 4 also shows a small change in the total diffusion zone volume between the two cases (12.28 compared to 13.23), which supports the previous conclusion that the heat leak was mainly due to axial conduction in the wall and not diffusion.

The condenser was sized using an emissivity of 0.80. Heat transfer was solely radiation to a sink temperature of ~ 14°C which corresponds to the approximate temperature of the water cooled jacket surrounding the radiator. The radiator geometry was designed to reject power from all four sides of the VCHP, including fins. The radiator sizing calculation took into account the view factor from the fins to the pipe and visa versa. Since the heat leak at the maximum temperature (370°C) is calculated to be 25 watts, the radiator was designed to reject the remaining power, or 785 watts.

Two fins were incorporated into the condenser as shown in Figure 5. Each fin was 17.00 inches long, 2.5 inches wide and 0.060 inches thick. The thickness was selected by comparing the condenser fin length versus condenser weight for several fin widths. In each case the condenser with fins was designed to reject 785 watts. The shortest fin length and the lowest mass was the preferred design. Reducing the overall length of the fin reduces the condenser effective length and thereby the liquid pressure drop for each groove.

Figure 6 shows a plot comparing the fin length and capillary pumping safety factor as a function of condenser mass. The capillary pumping safety factor is the maximum wick pumping capability divided by the sum of the vapor and liquid pressure drops at the design

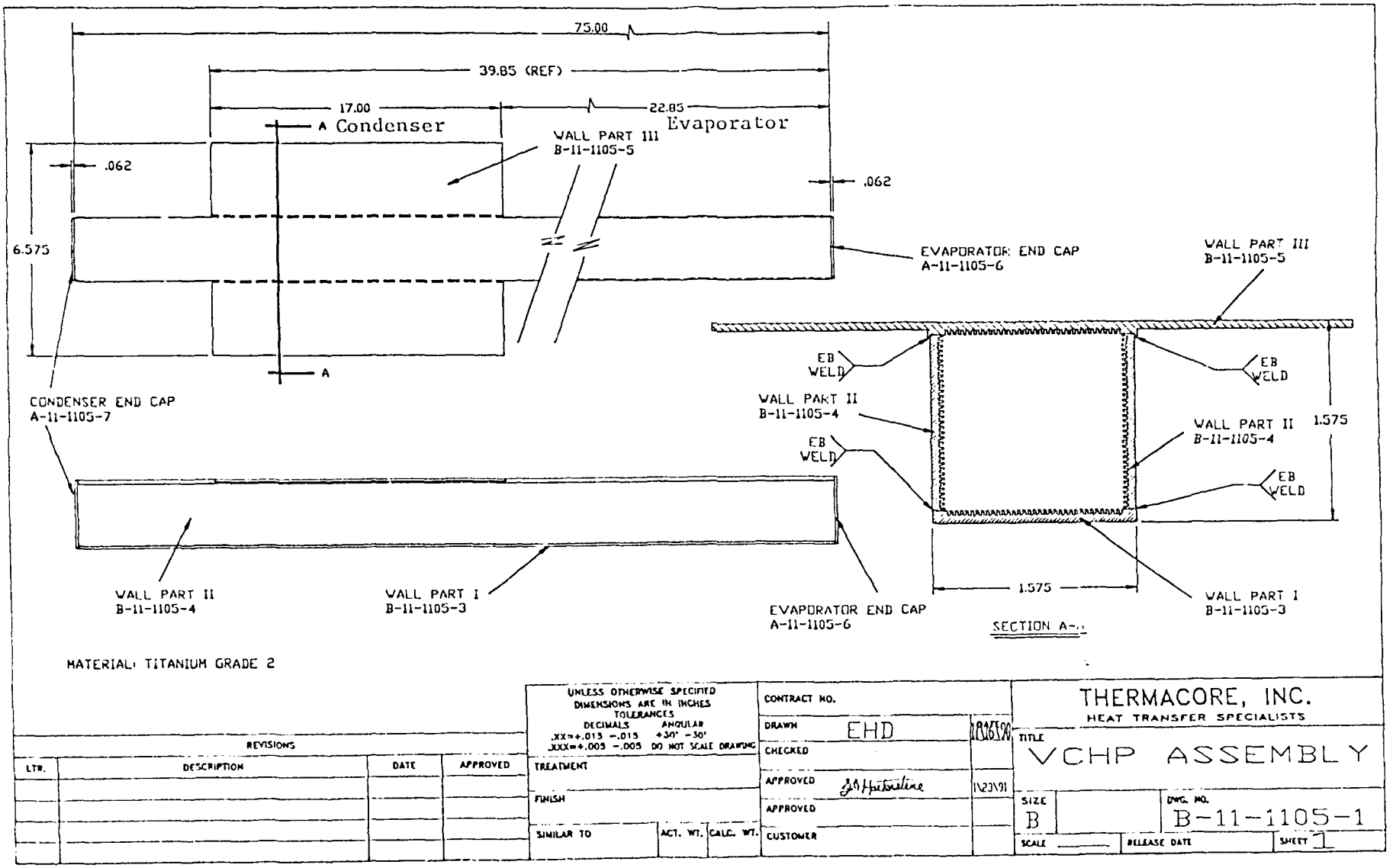

Figure 5. VCHP Assembly

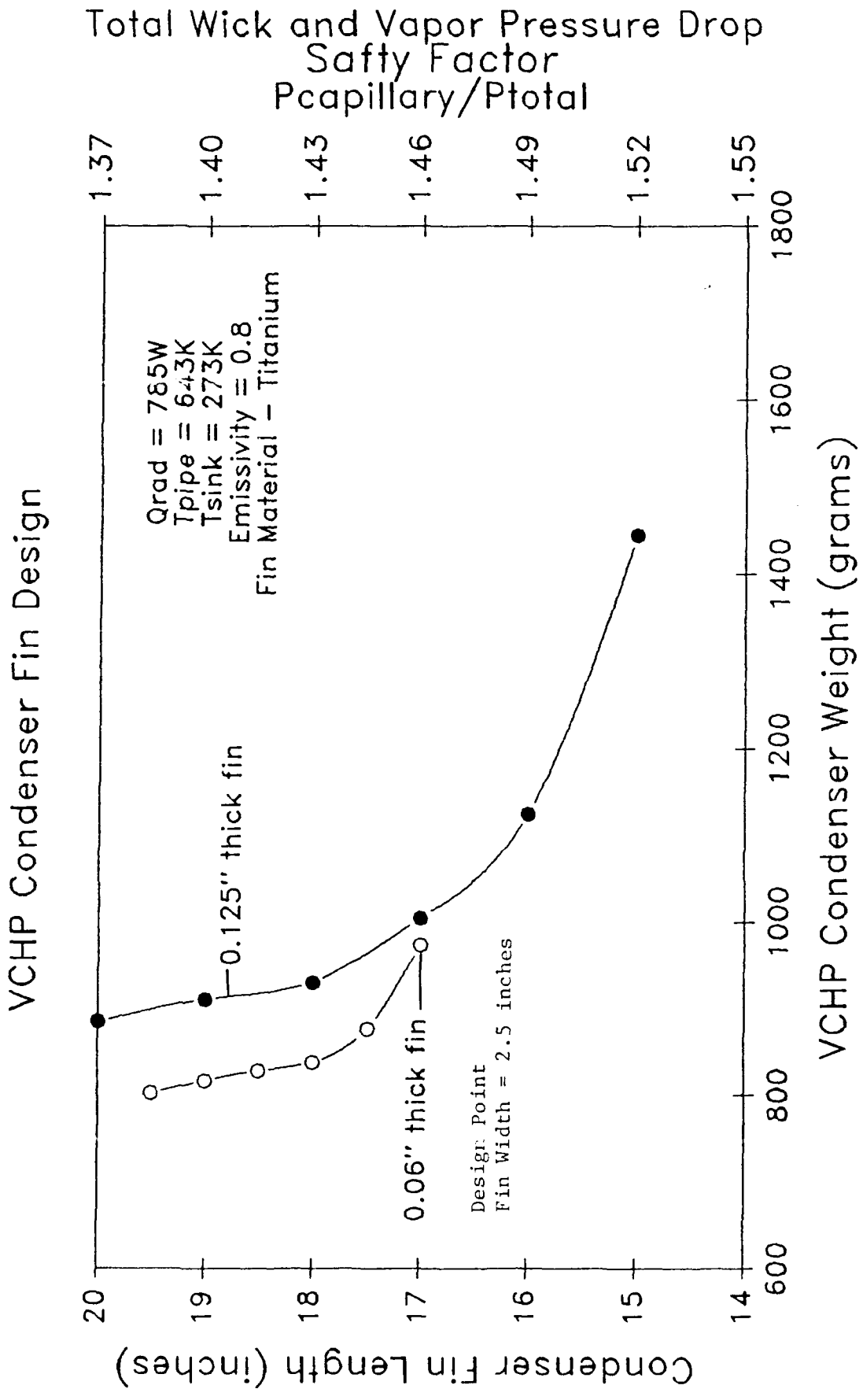

Figure 6. VCHP Condenser Fin Design

power condition. The 0.060 inch thick x 17.00 inch long x 2.5 inches wide fin was selected because it provides the lowest mass fin while having a 1.46 capillary pumping safety factor. Because of difficulties in machining titanium into thin sheet from plate stock, fin thicknesses less than 0.060 inches were not evaluated.

2.3 TASK 3: BATTERY CELL HEAT PIPE DESIGN

The role of the battery cell heat pipes (BCHP) is to transfer waste heat from the battery cells to the VCHP where the energy can be radiated to space. The BCHP's are mounted within the battery enclosure such that one BCHP can cool four (4) battery cells. In this section, the BCHP design will be discussed. The BCHP design parameters are listed in Table 5.

TABLE 5. Battery Cell Heat Pipe Design Parameters

Number of BCHP's	5
Wall Material	Titanium, CP-Grade 2
Working Fluid	Cesium
Evaporator Length	10.5 inches
Evaporator Geometry	1.00 inch outside diameter x 0.035 inch wall
Condenser Length	4.50 inches
Condenser Geometry	2.875 inch outside diameter x 0.083 inch wall
Wick Design (2 wraps)	Stainless steel screen 80 mesh
Power Rejected During Discharge	180 watts
Estimated Weight Per BCHP	1.0 lbs.

The BCHP evaporators transport the power from the battery cells to the BCHP condenser. The BCHP condenser was mounted onto the VCHP evaporator such that it surrounded the four walls of the VCHP (See Figure 7). Each BCHP vapor core is separate and distinct from the VCHP vapor core. The purpose of this integration geometry was to supply the power from the battery cells evenly to the VCHP evaporator. Since the wick design was

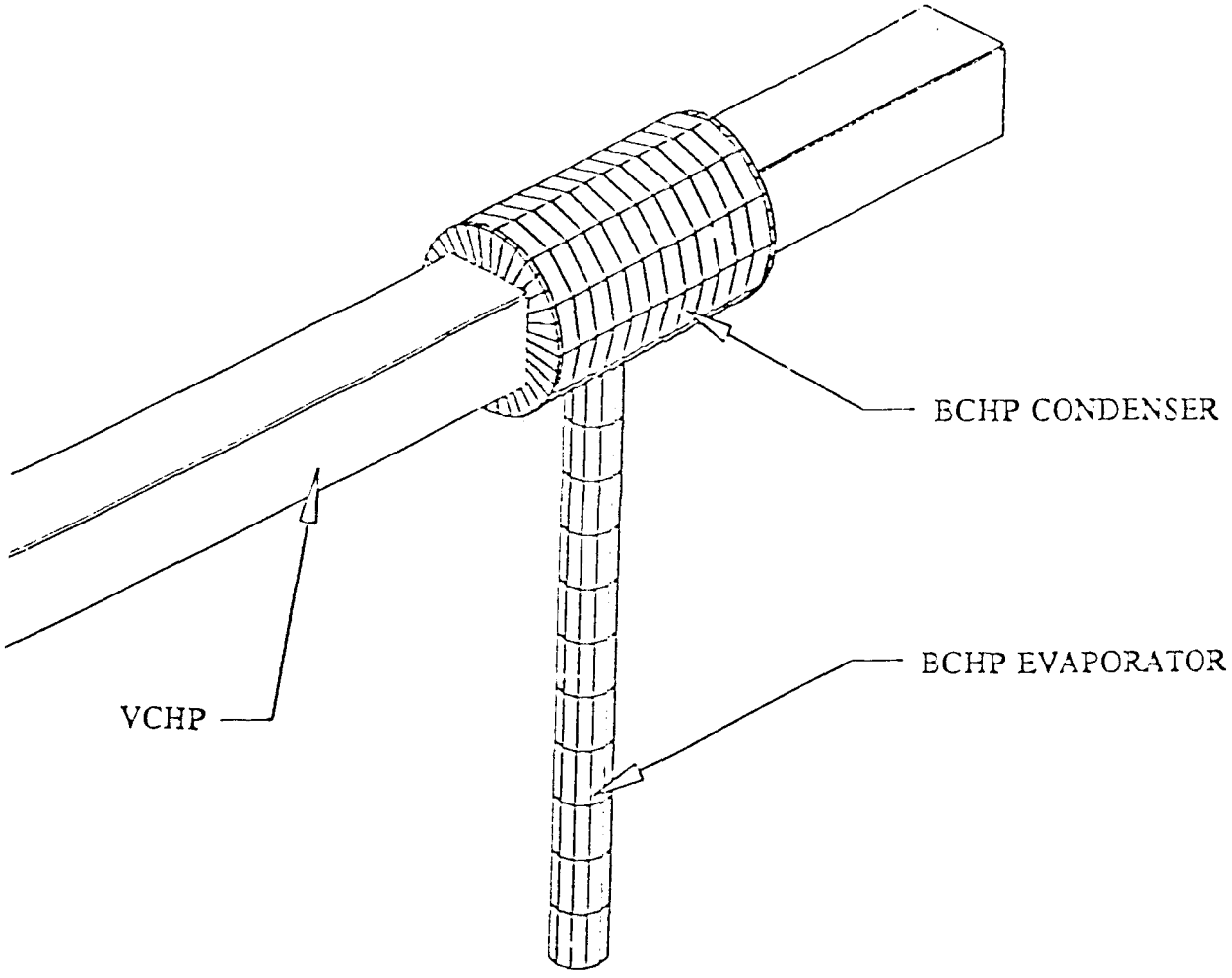

Figure 7. Battery Cell Heat Pipe Integration Concept with the Variable Conductance Heat Pipe

axial grooves, the power must be supplied on all four sides to fully utilize the axial groove capillary pumping capability.

The wick structure consisted of two (2) wraps of 80 mesh stainless steel screen instead of titanium screen. The reason for this change was the cost of the titanium screen. Titanium screen was quoted at over $400 per square foot from metal wire weaving manufacturers, and stainless steel was quoted at $6 per square foot. Because of the large amount of screen required ($\approx 14 ft^2$), stainless steel was chosen. Stainless steel has a similar thermal conductivity compared to titanium (21 W/m-K versus 19.5 W/m-K, respectively) and is proven compatible with cesium at elevated temperatures.[2] Therefore, this change should not impact the system reliability or performance.

Figure 8 shows the BCHP wick structure. The stainless steel screen was mounted on the inside diameter of both the evaporator and condenser walls as well as the outside surface area of the VCHP evaporator. Screen was also positioned between the VCHP and BCHP inner walls to provide a means of liquid return to the BCHP evaporator following condensation on the VCHP.

The BCHP was designed to operate either horizontally or gravity aided, with the evaporator down. The reason for this orientation is due to the low surface tension of cesium at 350°C and the associated low capillary pumping capability. The sum of the pressure drops will exceed the capillary pumping capability using wick designs without arteries. If operated against gravity, the gravitational pressure drop would exceed the capillary pumping capability causing BCHP dry out. This will not be an issue in space based operation due to the lack of gravity, however, a goal of the Phase II program will be to develop a BCHP wick structure that can reliably demonstrate operation against gravity on earth.

Initially, the BCHP evaporators were to include fins that would enhance the heat transfer from cartridge heaters simulating sodium-sulfur battery cells. Both the fins and the cartridge heaters were omitted because of the additional costs for materials and fabrication. Ceramic insulated heater cable was used in place of cartridge heaters to input power into the BCHP evaporator. The heater cable was wrapped circumferentially around the BCHP evaporator. This change was approved by WRDC (B. Hager) in a telephone conversation on January 3, 1991. The Phase II program will include, as one of the first tasks, the addition of fins onto the BCHP's fabricated in Phase I and the addition of cartridge heaters to simulate the battery cells.

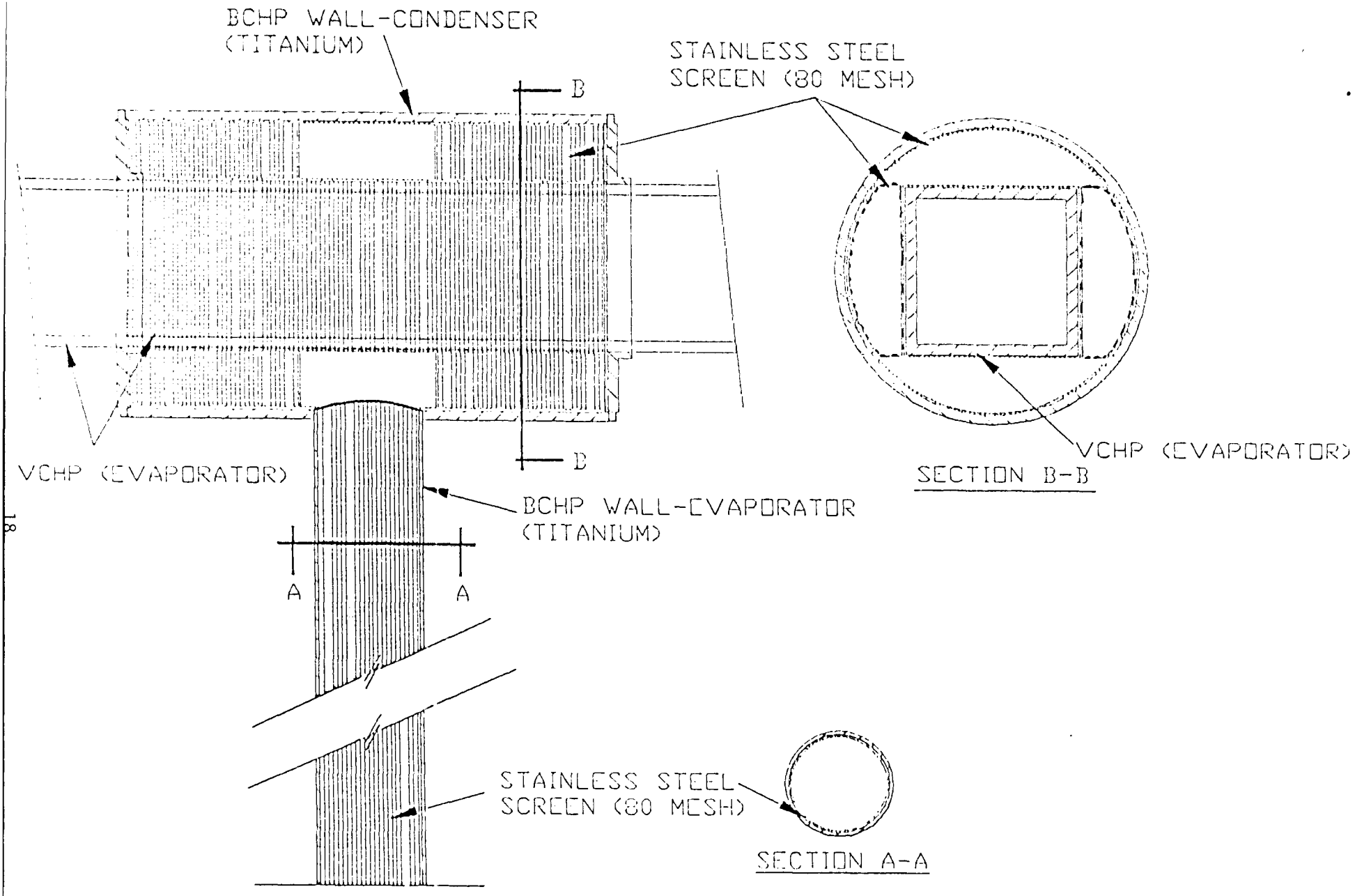

Figure 8. BCHP Wick Structure

2.4 TASK 4: VCHP/BCHP FABRICATION AND TEST

The fabrication and testing of the dual heat pipe assembly will be addressed in four sections as follows:

2.4.1 VCHP Fabrication

2.4.2 BCHP Fabrication

2.4.3 VCHP/BCHP Test Procedure

2.4.4 Test Results

2.4.1 VCHP Fabrication

The axial groove VCHP wick structure was machined integral into the titanium envelope wall. This task was performed by positioning the required number and size of milling machine cutters on an arbor and milling all of the grooves on one wall at the same time. 80 mesh titanium screen was spot-welded over the axial grooves to reduce the liquid pressure drop associated with the liquid counterflow shearing affect of vapor on the liquid surface. Figure 9 shows a photograph of the axial grooves and the axial grooves covered with titanium screen. The four walls of the VCHP were joined by electron beam welding. Figure 10 shows a photograph of the assembled VCHP.

2.4.2 BCHP Fabrication

The individual BCHP evaporators and condensers were welded together in an argon purged glove box to prevent oxygen from contaminating the weld area. Both the evaporator and condenser screen wicks were mounted to the BCHP walls by either spot welding or held in place with stainless steel springs. Photographs of the BCHP evaporator and condenser wicks are shown in Figures 11 and 12 respectively. A photograph of the assembled BCHP is shown is Figure 13.

Each of the five (5) BCHP's were welded onto the assembled VCHP by tungsten inert gas (TIG) techniques. The completed dual heat pipe assembly, shown in Figure 14, was checked for leaks using a helium mass spectrometer. Each of the BCHP's were individually charged with cesium and processed to remove unwanted noncondensible gas.

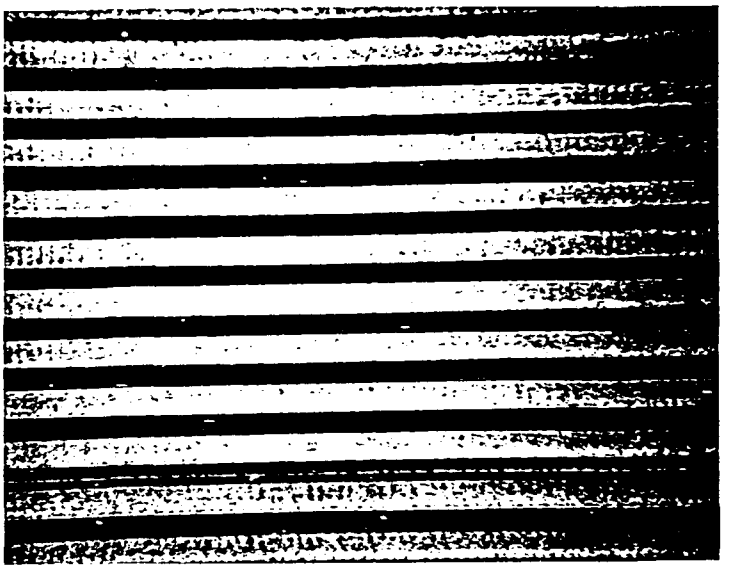

VCHP Axial Grooves

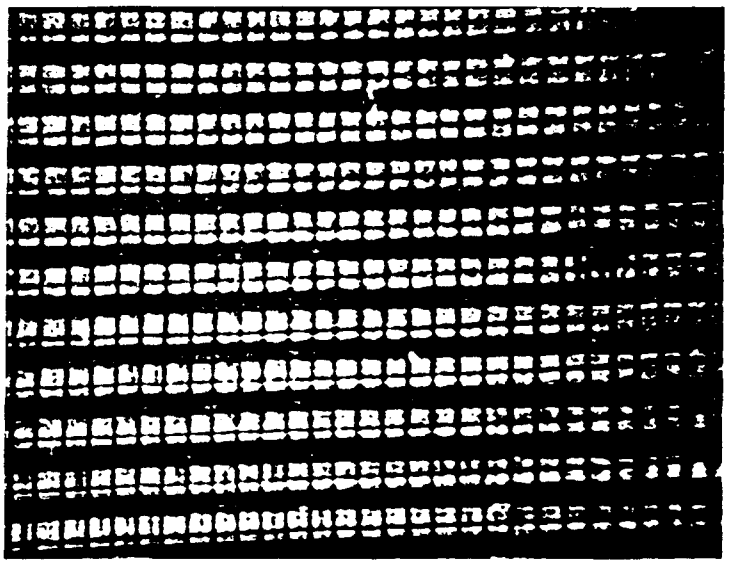

VCHP Axial Grooves Covered with
Titanium Screen

Figure 9. VCHP Wick Structure Photograph (8x Magnification)

Figure 10. VCHP Assembly Photograph

Figure 11. BCHP Evaporator Screen Wick

Figure 12. BCHP Condenser Screen Wick

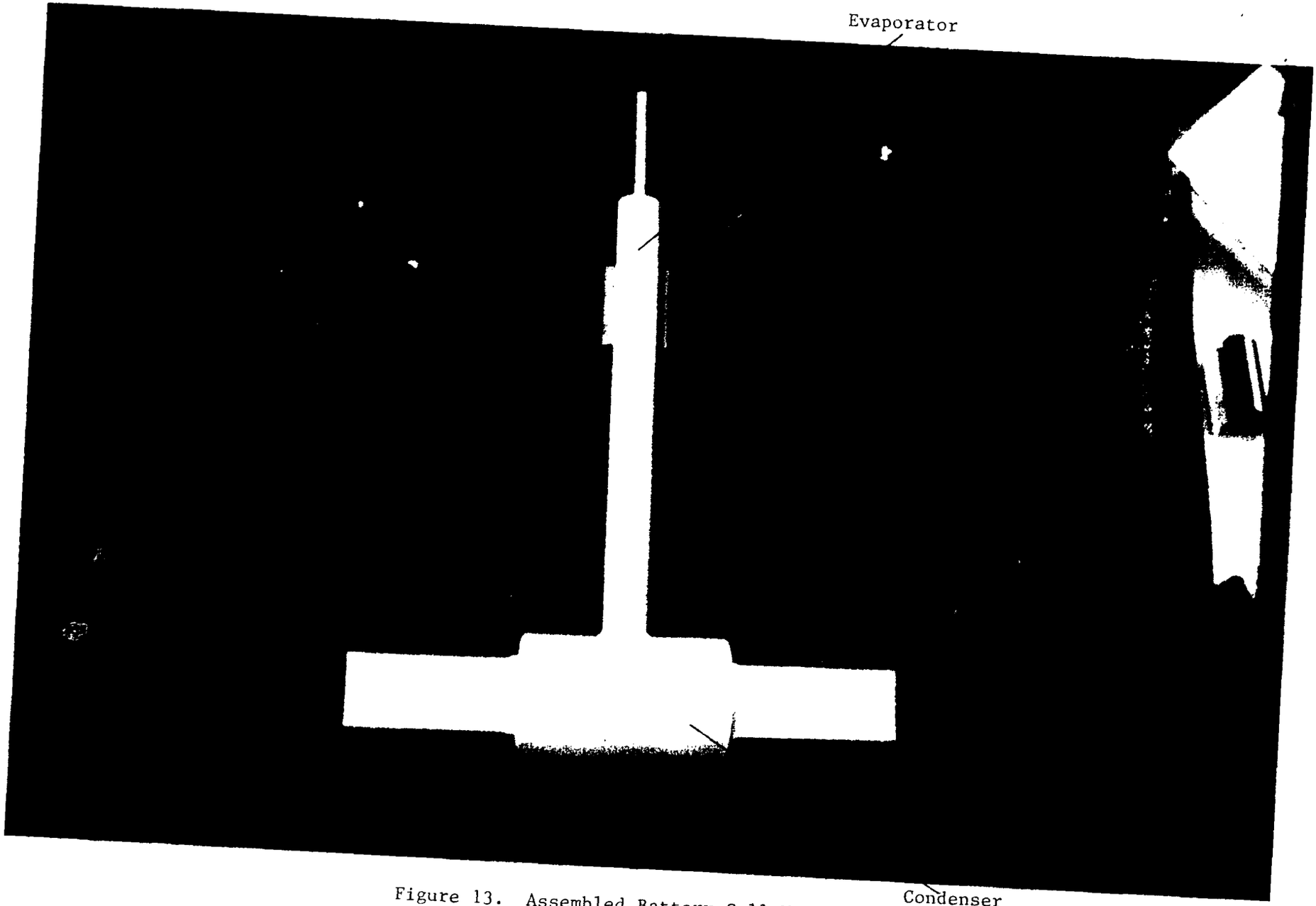

Figure 13. Assembled Battery Cell Heat Pipe

2.4.3 VCHP/BCHP Test Procedure

The VCHP and BCHP's were instrumented with twenty-six (26) type "K" thermocouples at locations shown in Figure 15. Cable heaters wrapped circumferentially around each individual BCHP evaporator provided the required power input to the VCHP.

The design emissivity of the VCHP condenser and reservoir was 0.80. Initially the VCHP was coated with a high temperature paint to meet this requirement, but initial performance tests yielded a lower than expected emissivity. As a result, the VCHP was coated with iron-titanate which has a documented emissivity of 0.87 at 815°C.[3] To determine the emissivity of this coating at 370°C, Thermacore fabricated a titanium/cesium heat pipe coated with iron-titanate. The heat pipe provided an isothermal surface from which to measure the temperature and calculate the surface emissivity. A built-in cartridge heater was mounted inside the heat pipe vapor space so that the electrical power input was equivalent to the power radiated from the surface. The test pipe was instrumented with two (2) type "K" thermocouples. With knowledge of the power radiated, the surface temperature and the area, the emissivity was calculated from the standard radiation equation. At 370°C an emissivity of 0.93 was measured.

The fully instrumented heat pipe assembly was mounted in the simulated battery enclosure and fixtured within a vacuum chamber. A water cooled calorimeter was mounted over the condenser and reservoir to measure the power radiated by measuring the delta-T in the water (T_{exit}-T_{inlet}) and the water flow. The VCHP was loaded with the required cesium volume and heated up to 400°C to remove the unwanted noncondensible gases. The required argon gas volume was then added to the VCHP.

To begin the performance test, the power input to the BCHP's was evenly increased until the power radiated from the VCHP radiator (measured by calorimetry) matched the LEO sodium-sulfur heat dissipation rate for 18 cells during recharge. This value reaches a minimum of 36 watts (18 cells x 2 watts/cell). The power was then increased and decreased at specified time intervals to match, as closely as practical, the profile of heat dissipation versus time for the battery cells during LEO recharge/discharge conditions. This profile is shown in Figure 2.

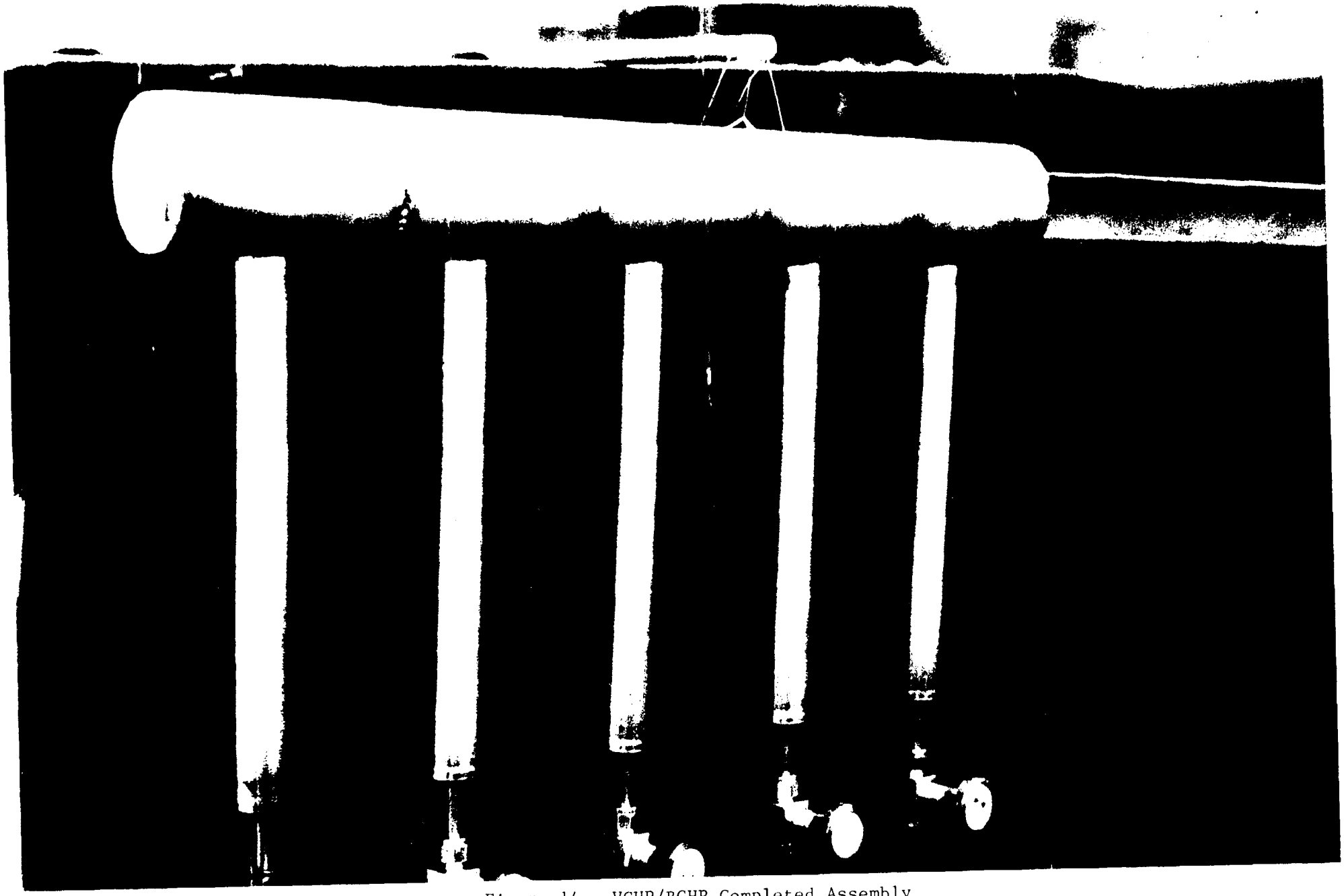

Figure 14. VCHP/BCHP Completed Assembly

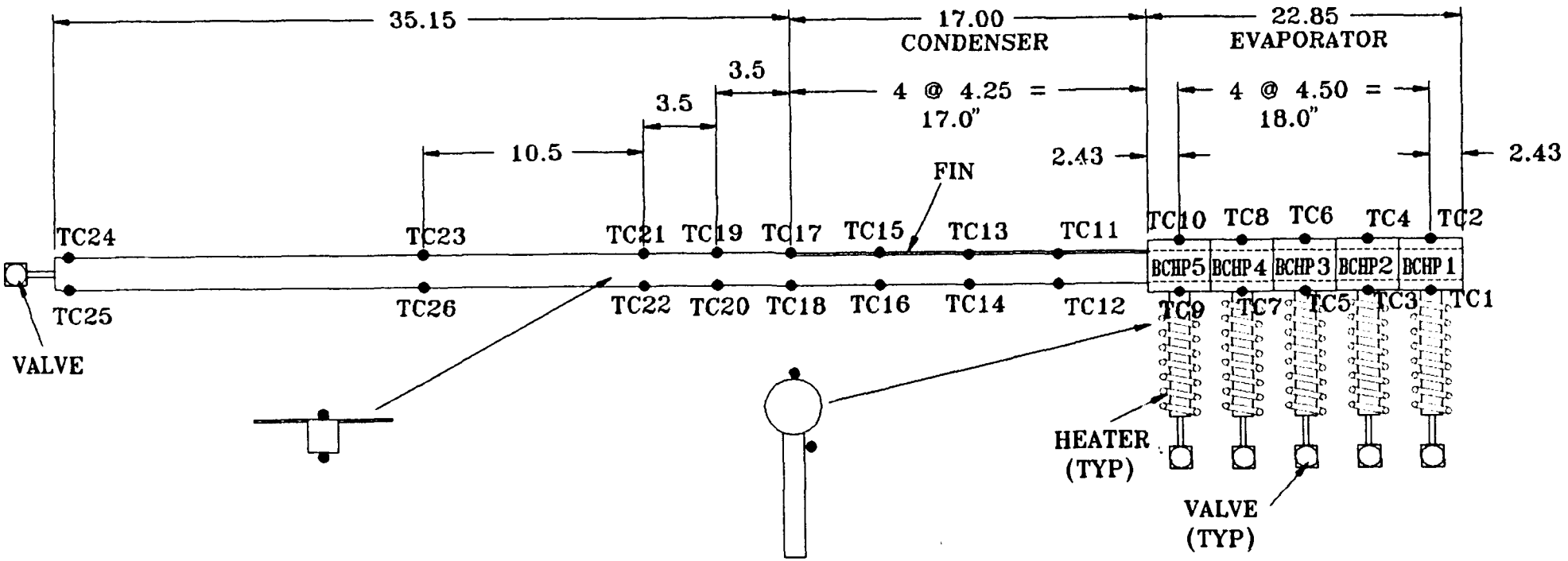

Figure 15.

VCHP / BCHP ASSEMBLY
THERMOCOUPLE AND HEATER LOCATION

C:\ACAD386\11-1106\25.DWG

2.4.4 Test Results

The VCHP temperature profile is shown in Figure 16 for the simulated cooling conditions of 18 sodium-sulfur battery cells during one orbital cycle. Three temperature profiles are plotted; 7 watts/cell (126 watts total), 35 watts/cell (630 watts total), and 45 watts/cell (810 watts total). The first profile occurs during recharge when the battery cells are dissipating 7 watts/cell. The lowest power level, 2 watts/cell, was not achieved following discharge within the required 20 minute time period because of the heat pipe's slow response time. At low power levels, the time response is slow due to the low vapor pressure of cesium at 350°C. Therefore, only 126 watts rejected was achieved within the first 20 minutes of recharge, and this value was maintained throughout the remaining 50 minutes of recharge.

The temperature profile during discharge is shown in the remaining two profiles; Q = 35 watts/cell, and Q = 45 watts/cell peak. The 35 watts/cell curve illustrates the VCHP concept of moving the noncondensible gas into the reservoir and exposing the condenser/radiator. The temperature control range between recharge (7 watts/cell) and discharge (35 watts/cell) was 24°C. Increasing the power to simulate the 45 watts/cell peak battery cell heat dissipation rate resulted in a 33°C temperature control range. The gas pocket was compressed further at this power level which exposed 5-6 inches of the reservoir for heat rejection.

The average temperature of the condenser during the 35 watts/cell discharge cycle was 360°C and the total radiated power was 627 watts. This corresponds into a 0.7 combined VCHP and calorimeter emissivity. A combined emissivity of 0.8 is required. This lower than expected value caused the temperature control range to be 13°C higher than the 20°C design point.

The power radiated from the heat pipe and transferred to the water cooled calorimeter is a function of their respective emissivities and geometry as expressed by the following equation:

$$q_{VCHP\text{-}calorimeter} = \frac{\sigma A (T_p^4 - T_{cal}^4)}{\frac{1}{\epsilon_{VCHP}} + \frac{1-\epsilon_{cal}}{\epsilon_{cal}} (\frac{r_{VCHP}}{r_{cal}})}$$

nasvchp.dsf/nasvchp5.grf June 27, 1991 9:29:38 AM

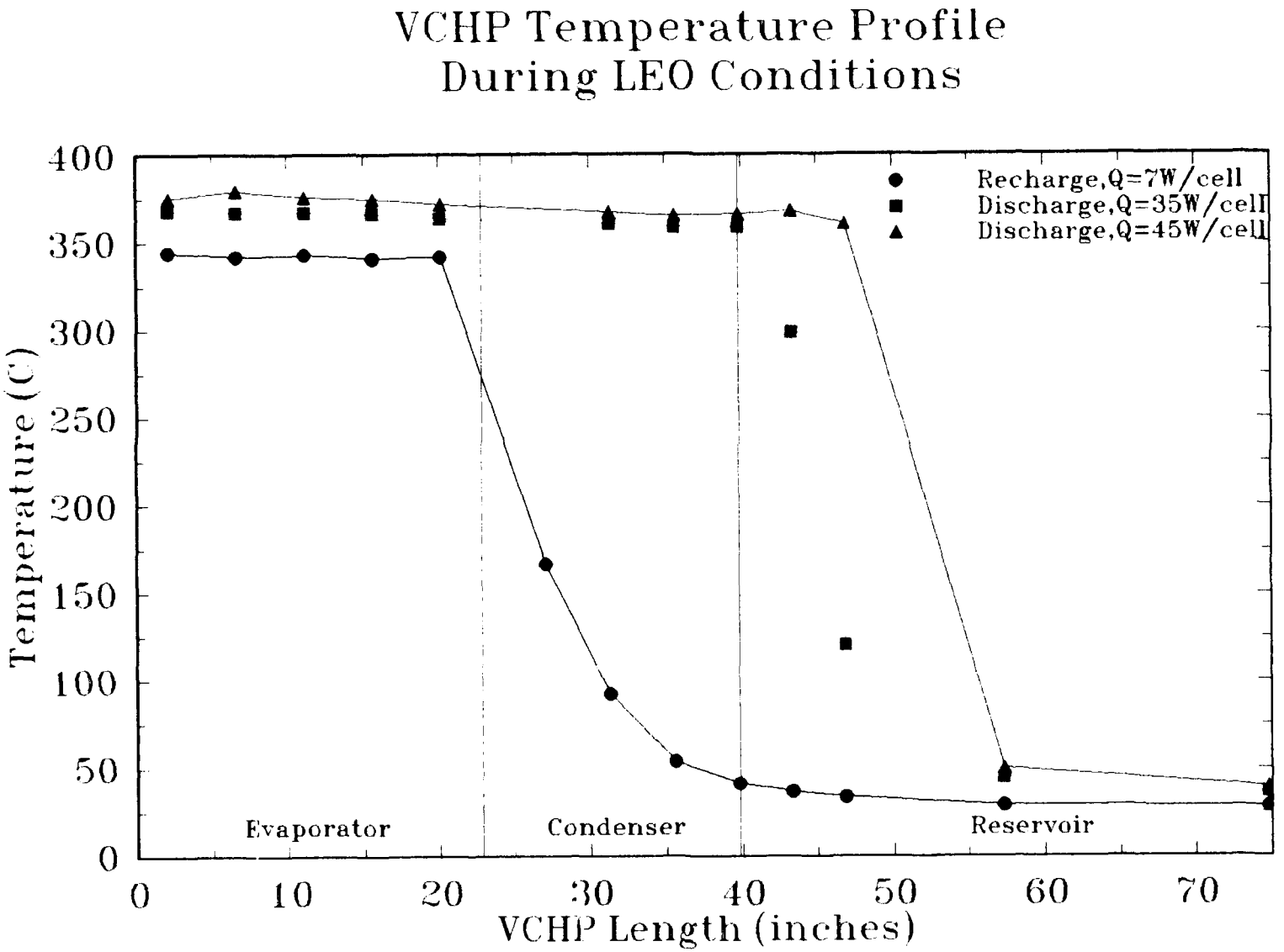

Figure 16. VCHP Temperature Profile During LEO Conditions

Where:

σ = Stephan-Boltzman Constant $\equiv 5.67 \times 10^{-8}$ W/m^2-K^4

A = radiating area of the VCHP (m^2)

T_p = VCHP temperature (K)

T_{cal} = Calorimeter temperature (K)

ϵ_{VCHP} = VCHP emissivity

ϵ_{cal} = calorimeter emissivity

r_{VCHP} = radius of the VCHP

r_{cal} = radius of the calorimeter

It is assumed that the VCHP is circular in geometry with a diameter that corresponds to the width of the four VCHP walls (2.00 inches diameter). The diameter of the calorimeter was 10 inches. The remaining variables were taken from data during test.

Figure 17 shows a plot of the VCHP versus the calorimeter emissivity for the radiator operating at 360°C and radiating 630 watts. The plot indicates that a combined emissivity of 0.7 is required to meet the 360°C temperature and 630 watt power requirement. If the emissivity of the VCHP was 0.93 as demonstrated earlier on a test heat pipe, the resulting calorimeter emissivity was 0.305 or if the VCHP emissivity was 0.7, the resulting calorimeter emissivity was 0.95.

The VCHP performed as designed with the exception of the higher than predicted temperature control range attributed to a lower than expected emissivity. Emissivity coatings are highly sensitive to process controls such as pre-cleaning, surface preparation (sand-blasting), application methods, handling, quality of coating material from lot-to-lot and coating thickness. In Phase II, Thermacore will improve these controls internally and with coating vendors to achieve a consistent combined emissivity of 0.8.

Figure 18 shows the power radiated from the VCHP during two (2) simulated orbital cycles. During the first cycle radiated power was lower because the power input into the BCHP's was selected by trial-and-error because of the uncertainty of the radiative losses in the vacuum system. The power improved during the second cycle, indicating that the discharge power levels were almost met withir the given discharge time period. The heater power was

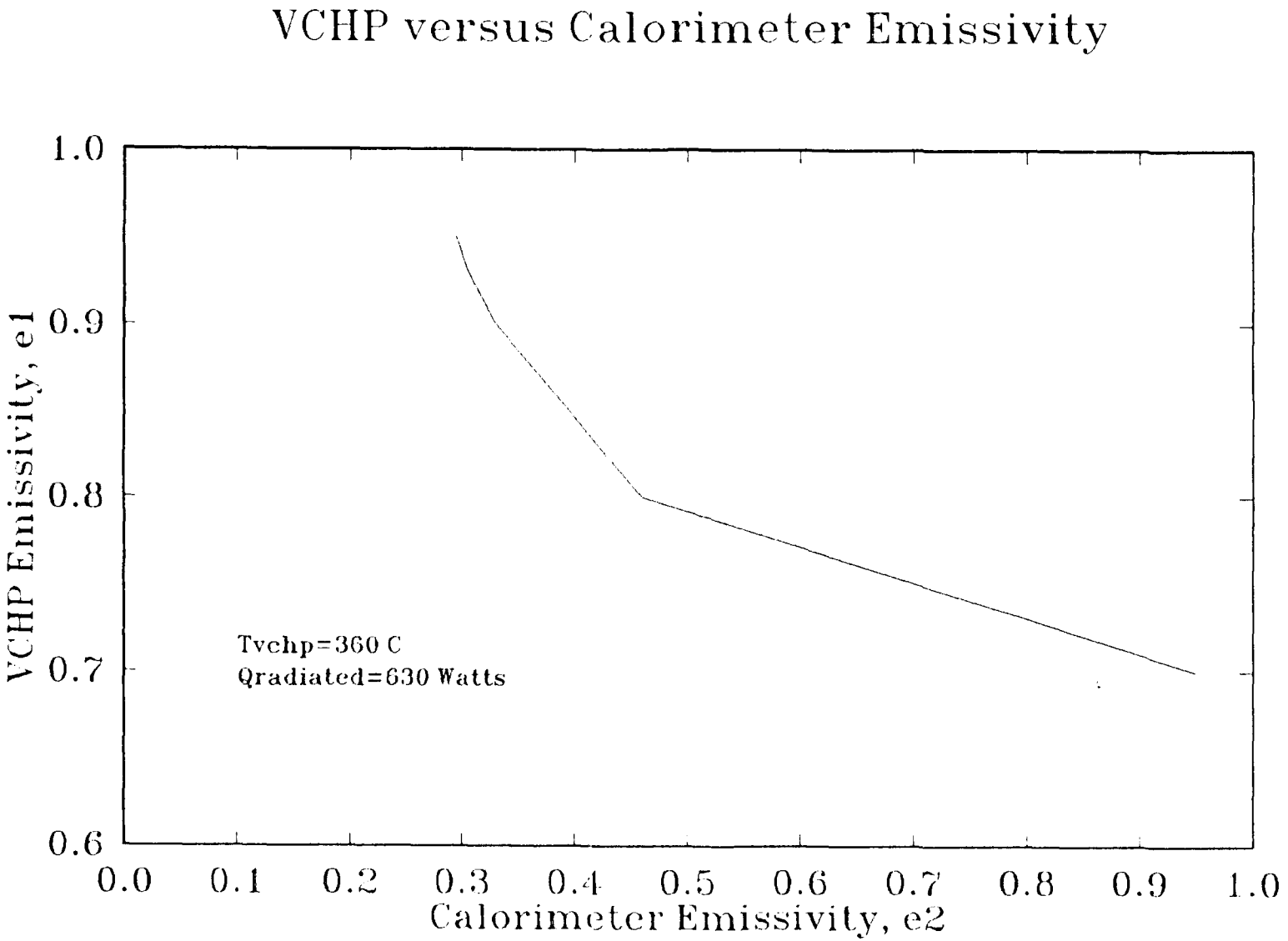

Figure 17. VCHP Versus Calorimeter Emissivity

nasqtime.dsf/nasqtim1.grf June 27, 1991 9:30:36 AM

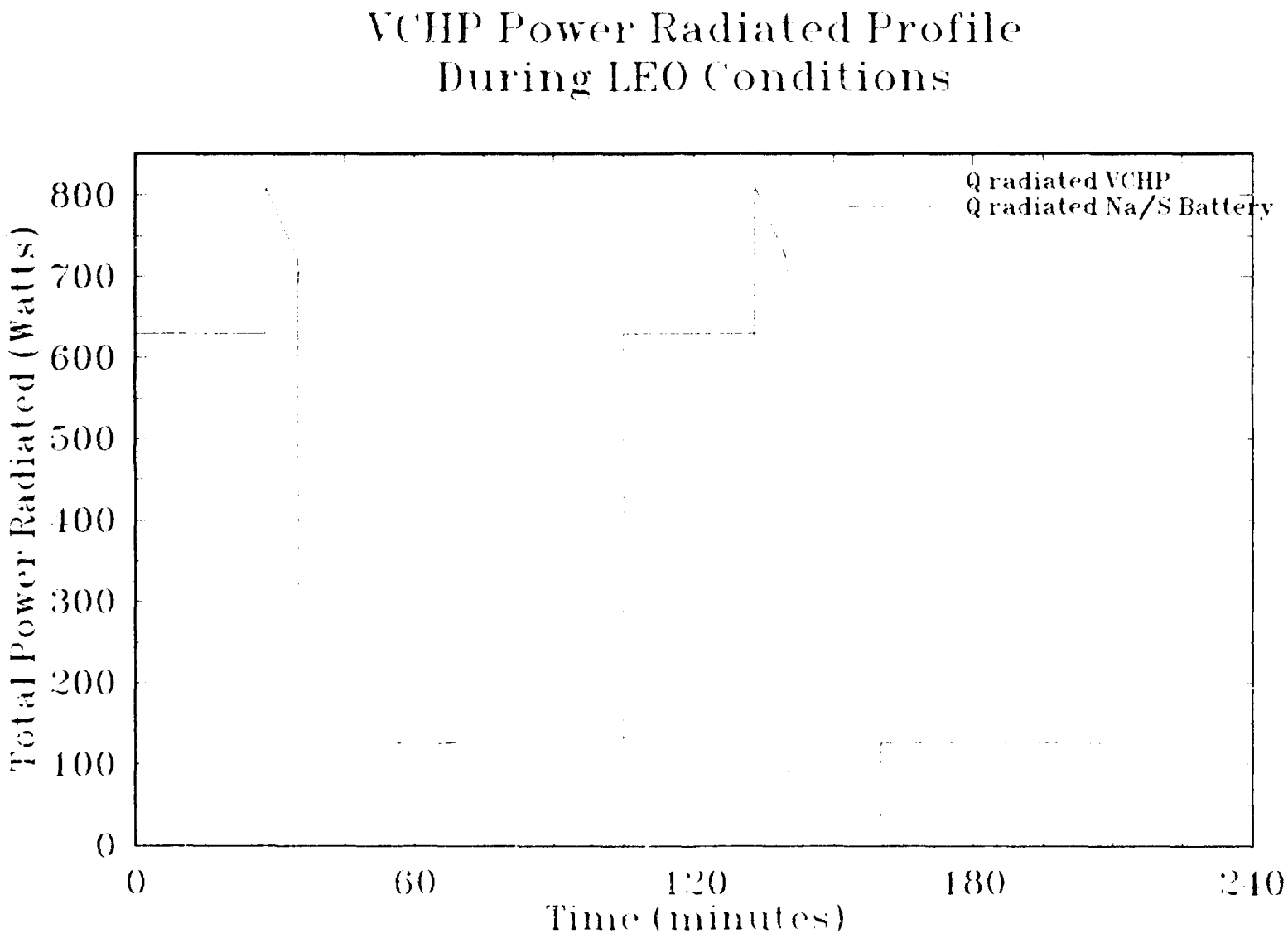

Figure 18. VCHP Power Radiated Profile During LEO Conditions

increased and decreased at specified time intervals corresponding to the sodium-sulfur battery LEO conditions. Even though the power was decreased to the recharge power level, the VCHP continued to increase its radiative losses due to the thermal mass of the pipe.

Table 6 documents the battery cell heat pipe delta-T between the evaporator and condenser at Q = 7 watts/cell and Q = 45 watts/cell heat dissipation conditions. At the Q = 7 watts/cell condition the delta-T ranged from 1°C to 9°C. At the Q = 45 watts/cell condition the delta-T ranged from 3°C to 50°C. The cause of the large delta-T's in some of the heat pipes is attributed to unwanted noncondensible gas present in the vapor core. The gas blocks the condenser region and causes the evaporator to operate at a higher temperature than desired. Most likely the gas leaked into the heat pipes at the fittings connecting the fill tube valves to the fill tubes. These fittings are rated for 150°C service, but can be effectively operated at higher temperatures for a short period of time.

TABLE 6. Battery Cell Heat Pipe Delta-T (°C)

	Q = 7 watts/cell			Q = 45 watts/cell		
	Evaporator	Condenser	ΔT	Evaporator	Condenser	ΔT
BCHP 1	344	345	1	426	376	50
BCHP 2	351	342	9	405	380	25
BCHP 3	343	343	--	381	376	5
BCHP 4	352	341	9	395	375	20
BCHP 5	342	342	--	375	372	3

The continual testing at 350°C decreased the integrity of the fittings allowing gas to penetrate into the pipe. This is further substantiated by the continual increase in heat pipe delta-T's as testing progressed. Initial testing indicated a 1°C delta-T in the BCHP's. Welded connections without values are planned for production heat pipes.

The internal generation of noncondensible gas caused by reactions between the envelope and fluid materials is not probable because of the range in delta-T's (50°C to 3°C) between the 5 BCHP's. If a materials incompatibility existed, all 5 heat pipes would have a similarly high delta-T. In Phase II, the BCHP's will be re-processed to remove the gas and welded closed to reduce the probability of leaks.

3.0 CONCLUSIONS AND RECOMMENDATIONS

The primary objective of this Phase I program was to demonstrate the thermal management of sodium-sulfur batteries using interchangeable variable conductance heat pipes and constant conductance heat pipes. The objectives of this program were successfully met in every aspect as demonstrated by eight (8) titanium/cesium heat pipes fabricated in direct technical support of this program. The specific conclusions are as follows:

- A 24°C temperature control range was demonstrated as the heat load from the battery cells increased from 7 watts/cell (recharge) to 35 watts/cell (discharge). A 33°C temperature control range was demonstrated as the heat load further increased from 35 watts/cell to an instantaneous peak power of 45 watts/cell.
- A lower than expected combined emissivity between the VCHP radiator and the water cooled calorimeter is the cause of the measured temperature control range exceeding the 20°C design value. Analysis of the data yielded a combined emissivity of 0.7 which was less than the 0.8 design goal.
- The development of the dual heat pipe assembly demonstrated the ability of five (5) constant conductance heat pipes with separate distinct vapor cores to efficiently supply power to a single variable conductance heat pipe.
- The primary component of the heat leak is axial conduction in the VCHP wall and not the diffusion of cesium into the reservoir as originally hypothesized.
- The dual heat pipe assembly was successfully fabricated without major design or procedural changes, demonstrating the ease of fabrication that will be carried over into Phase II.
- A total BCHP/VCHP weight of 6164 grams (13.5 lbs) was measured. This weight can be reduced to less than 3150 grams (6.9 lbs.) in Phase II by substituting conventional circular tubing instead of the square tubing used in Phase I.

Based on these conclusions it is apparent that the dual heat pipe concept to cool sodium-sulfur batteries is readily achievable as demonstrated by performance testing the six (6) heat pipe

assembly. Since the heat pipe concept has been proved, Phase II work will focus on fabricating a lightweight BCHP/VCHP assembly for testing in actual sodium-sulfur batteries supplied by Eagle Picher, Joplin, Missouri. Specifically, the recommendations for Phase II are as follows:

- Update thermal, electrical and geometric parameters for LEO sodium-sulfur batteries.
- Continue testing the heat pipe assembly fabricated in Phase I using cartridge heaters to simulate the sodium-sulfur battery cells. Incorporate fins onto the BCHP's to enhance the heat transfer from the cartridge heaters to the BCHP evaporators.
- Address risk assessment issues to determine the effect of meteoroids and space debris on the VCHP radiator.
- Modify the square VCHP geometry into a circular geometry and identify lightweight envelope and fin materials to produce a lightweight thermal management package.
- Fabricate and test the lightweight dual heat pipe assembly in actual sodium-sulfur batteries.
- Determine the impact on weight and design if survivability requirements are imposed on the heat pipes.

4.0 REFERENCES

1. Schlitt, K.R., Brennan, P.J. Kirkpatrick, J.P., "Parametric Performance of Extruded Axial Grooved Heat Pipes from 100°K to 300°K," AIAA Paper No. 74-724, AIAA/ASME 1974 Thermophysics and Heat Transfer Conference.

2. J.J. Moscony, "The Compatibility of Cesium with Electron Tube Materials," Radio Corporation of America, Lancaster, Pennsylvania, Page 13, August 24, 1962.

3. Cleary, R.E., Emanuelson, R., Luoma, W., Ammann, C., "Properties of High Emittance Materials", NASA-CR-1278, Prepared by United Aircraft Corporation, East Hartford, CT, February 1969.

APPENDIX A

VARIABLE CONDUCTANCE HEAT PIPE DIFFUSION MODEL

Title: Derivation of VCHP Diffusion Equations

Project: 1-1105

Calculated by: [illegible] Date: 12/3/92
Checked by: [illegible] Date: 2/18/91
Reviewed by: Date:

Purpose: To derive equations and their finite-difference approximations for the calculation of the cesium concentration and vapor space temperature in the diffusion region of a variable conductance heat pipe.

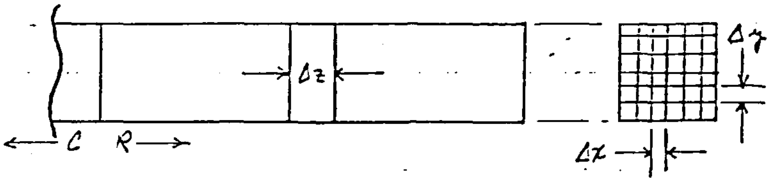

Analysis:

Boundary conditions:

@ cond./reservoir interface ($z=0$) : $C = \rho_{cesium\ vapor\ @\ 643\ K}$ (i.e. no argon)

$T = 643\ K$

@ vapor space/wall interface : $T_{vapor\ mixture} = T_{wall}$

@ end of reservoir : $\nabla T = 0$ (axially) $\left[\frac{\partial T}{\partial z} = 0\right]$

The concentration profile is derived from a mass balance on a differential element:

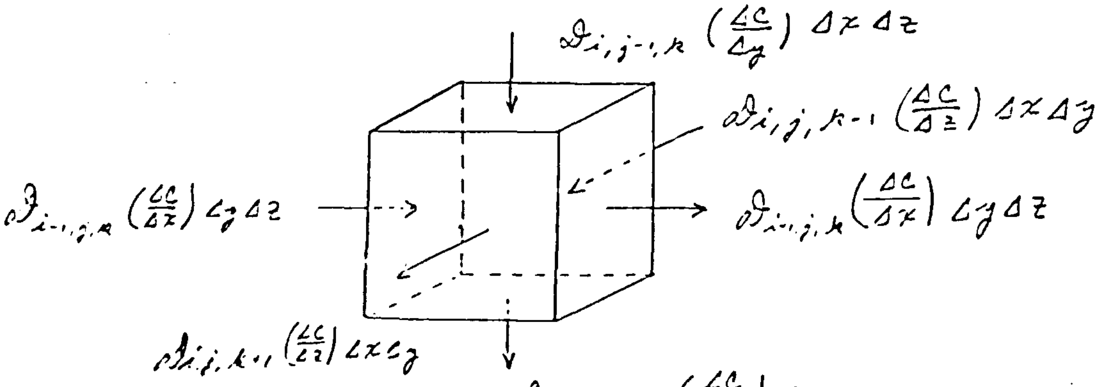

Title: Derivation of VCHP Diffusion Eq. Terms
Project: 11-1105
Calculated by: J. Rogers Date: 12/3/90
Checked by: R.F. Boehm Date: 2/14/91
Reviewed by: _____ Date: _____

Basically, mass into the element must equal the mass out of the element:

$$\mathcal{D}_{A,i-1,j,k}\left(\frac{C_{i-1,j,k}-C_{i,j,k}}{\Delta x}\right)\Delta y\,\Delta z+\mathcal{D}_{A,i+1,j,k}\left(\frac{C_{i+1,j,k}-C_{i,j,k}}{\Delta x}\right)\Delta y\,\Delta z$$

$$+\mathcal{D}_{A,i,j-1,k}\left(\frac{C_{i,j-1,k}-C_{i,j,k}}{\Delta y}\right)\Delta x\,\Delta z+\mathcal{D}_{A,i,j+1,k}\left(\frac{C_{i,j+1,k}-C_{i,j,k}}{\Delta y}\right)\Delta x\,\Delta z$$

$$+\mathcal{D}_{A,i,j,k-1}\left(\frac{C_{i,j,k-1}-C_{i,j,k}}{\Delta z}\right)\Delta x\,\Delta y+\mathcal{D}_{i,j,k-1}\left(\frac{C_{i,j,k-1}-C_{i,j,k}}{\Delta z}\right)\Delta x\,\Delta y$$

$$=0$$

Divide both sides by the element volume, $(\Delta x)(\Delta y)(\Delta z)$, to get:

$$\mathcal{D}_{A,i-1,j,k}\left[\frac{C_{i-1,j,k}-C_{i,j,k}}{(\Delta x)^2}\right]+\mathcal{D}_{A,i+1,j,k}\left[\frac{C_{i+1,j,k}-C_{i,j,k}}{(\Delta x)^2}\right]$$

$$+\mathcal{D}_{A,i,j-1,k}\left[\frac{C_{i,j-1,k}-C_{i,j,k}}{(\Delta y)^2}\right]+\mathcal{D}_{A,i,j+1,k}\left[\frac{C_{i,j+1,k}-C_{i,j,k}}{(\Delta y)^2}\right]$$

$$+\mathcal{D}_{A,i,j,k-1}\left[\frac{C_{i,j,k-1}-C_{i,j,k}}{(\Delta z)^2}\right]+\mathcal{D}_{A,i,j,k+1}\left[\frac{C_{i,j,k+1}-C_{i,j,k}}{(\Delta z)^2}\right]=0$$

where $\mathcal{D}_{A,i,j,k}$ denotes an average of the diffusion coefficients for nodes $(i+1,j,k)$ and (i,j,k). $\mathcal{D}_A$ is temperature dependent:

$$\mathcal{D}_A \propto T^{3/2} \qquad (T \text{ in absolute units})$$

Title: Derivation of VCHP Diffusion Equations
Project: 11-1105
Calculated by: D. Bugat Date: 12/7/90
Checked by: T. Anderson Date: 1/14/91
Reviewed by: _____ Date: _____
Page 3 of 4

The nodal temperature is determined from an energy balance on the differential element. I will first present it one-dimensionally, then expand it to 3 spatial dimensions.

Heat transport in the vapor will be primarily from mass flow and conduction. Natural convection will be ignored because the total pressure is assumed to be constant. Forced convection will be ignored because the flow velocities are very low.

The one-dimensional case is then: (x-direction)

$$\left[D_{A,i-1,j,k}\left(\frac{C_{i-1,j,k}-C_{i,j,k}}{\Delta x}\right)\Delta y\,\Delta z\right] C_{p_A,i-1,j,k}\left(T_{i-1,j,k}-T_{i,j,k}\right)$$

$$-\left[D_{A,i+1,j,k}\left(\frac{C_{i+1,j,k}-C_{i,j,k}}{\Delta x}\right)\Delta y\,\Delta z\right] C_{p_A,i+1,j,k}\left(T_{i+1,j,k}-T_{i,j,k}\right)$$

$$+k_{A,i-1,j,k}\left(\frac{T_{i-1,j,k}-T_{i,j,k}}{\Delta x}\right)\Delta y\,\Delta z+k_{A,i+1,j,k}\left(\frac{T_{i+1,j,k}-T_{i,j,k}}{\Delta x}\right)\Delta y\,\Delta z$$

$$=0$$

Where: C_{p_A} ≡ average specific heat; function of mass fraction

k_A ≡ average thermal conductivity; function of mole fraction and Temperature

This equation is rather long in one-dimension. To make it easier to work with, divide both sides by $(\Delta x)(\Delta y)(\Delta z)$ and define:

Title: Derivation of UCHP Diffusion Equations
Project: 11-1105
Calculated by: J. Sargent Date: 2/2/90
Checked by: [illegible] Date: 2/14/91
Reviewed by: _____ Date: _____

$$A_{i-1,j,k} = D_{A,i-1,j,k}\left(\frac{C_{i-1,j,k} - C_{i,j,k}}{(\Delta x)^2}\right) C_{PA,i-1,j,k}\,(T_{i-1,j,k} - T_{i,j,k})$$

The equation in 3 spatial dimensions is then:

$$A_{i-1,j,k} - A_{i+1,j,k} + A_{i,j-1,k} - A_{i,j+1,k} + A_{i,j,k-1} - A_{i,j,k+1}$$

$$+ k_{A\,i-1,j,k}\left[\frac{T_{i-1,j,k} - T_{i,j,k}}{(\Delta x)^2}\right] + k_{A,i+1,j,k}\left[\frac{T_{i+1,j,k} - T_{i,j,k}}{(\Delta x)^2}\right]$$

$$+ k_{A,i,j-1,k}\left[\frac{T_{i,j-1,k} - T_{i,j,k}}{(\Delta y)^2}\right] + k_{A,i,j+1,k}\left[\frac{T_{i,j+1,k} - T_{i,j,k}}{(\Delta y)^2}\right]$$

$$+ k_{A,i,j,k-1}\left[\frac{T_{i,j,k-1} - T_{i,j,k}}{(\Delta z)^2}\right] + k_{A,i,j,k+1}\left[\frac{T_{i,j,k+1} - T_{i,j,k}}{(\Delta z)^2}\right]$$

$$= 0$$

The mixture thermal conductivity is determined by calculating the number of moles of cesium and argon in each cell from the current cesium concentration value and then using the Mason and Saxena modification to the Wassiljewa equation as described in:
The Properties of Gases and Liquids, 4th edition, pp. 530-532; by Reid, Prausnitz, and Poling, McGraw-Hill Book Company, New York, 1987.